JOURNAL OF AGRICULTURAL AND FOOD CHEMISTRY

Using ATR-FTIR Spectroscopy To Design Active Antimicrobial Food Packaging Structures Based on High Molecular Weight Chitosan Polysaccharide

JOSÉ M. LAGARON,*,† PATRICIA FERNANDEZ-SAIZ,† AND MARIA J. OCIO†,‡

Novel Materials and Nanotechnology, Institute of Agrochemistry and Food Technology (IATA), CSIC, Apartado Correos 73, 46100 Burjassot, Spain, and Department of Preventative Medicine, Faculty of Pharmacy, University of Valencia, 46100 Burjassot, Spain

ATR-FTIR spectroscopy has been used in this study to characterize the molecular mechanisms and kinetic processes that take place when a chitosonium acetate thin coating is put in contact with water solutions, *Staphylococcus aureus* solutions, microbial nutrient solutions, and with a high water activity TSA hydrogel medium to simulate the effect of direct contact with high moisture foods such as fresh meats, fish, and seafood products or beverages. The results of this work suggest that the biocide carboxylate groups that form when chitosan is cast from acetic acid solutions are being continuously evaporated from the formed film in the form of acetic acid (mechanism I) in the presence of environmental humidity, rendering weak biocide film systems. On the other hand, upon direct contact of the cast chitosonium acetate film with liquid water, water solutions, or the high moisture TSA hydrogel, a positive rapid migration, with a diffusion coefficient faster than 3.7×10^{-12} m^2/s, of protonated glucosamine water soluble molecular fractions (mechanism II) takes place from the film into the liquid phase, yielding strong antimicrobial performance and leaving in the remaining cast film only the non-water soluble chitosan fractions. Finally, this study describes a refined spectroscopic methodology to predict the antimicrobial properties of chitosan and gives insight into the capacity of chitosan as a natural biocide agent.

KEYWORDS: Chitosan; active packaging; antimicrobial packaging; FTIR

INTRODUCTION

Research into the area of antimicrobial active food packaging materials has increased significantly during the past few years as an alternative method to control undesirable microorganisms on foods by means of the incorporation of antimicrobial substances in or coated onto the packaging materials (*1*−*3*). Since microbial contamination of most foods occurs primarily at the surface due to post-processing handling, it is appropriate to design antimicrobial systems that can act by direct contact or, more desirably, that can undergo positive migration from the package structure into the foods to reach potential inner contamination (*1*). The major potential food applications for antimicrobial films include meat, fish, poultry, bread, cheese, fruits, vegetables, and beverages (*4*, *5*).

Chitosan (*β*-(1,4)-2-amino-2-deoxy-D-glucose) is a biodegradable, biocompatible, prebiotic, and fat retaining edible aminopolysaccharide obtained by deacetylation of chitin, which is one of the worlds' most abundant biopolymers. Chitosan has also been reported to make no impact on the quality properties of foods and has excellent film and coating forming properties when cast from organic acidic water solutions (*6*). While it has been widely reported that this material has proven to have antimicrobial properties against bacteria, yeasts, and fungi (*7*−*9*), the mechanisms of action and film forming conditions that provide chitosan and chitosan derivatives with optimum biocide performance are still a matter of debate (*7*−*15*). It has been suggested that the polycationic nature of this biopolymer that forms from organic acidic solutions below pH 6.5 is a crucial factor (*9*−*13*). More recent research (*16*) indicates that only water insoluble chitosan in organic acidic solutions (i.e., chitosonium salts) appears to have efficient biocide properties. Previous work carried out in our group using FTIR spectroscopy assessed the film forming properties and chemical structure of different formulations of high molecular weight chitosan and correlated the structure of the material with its antimicrobial properties (*17*).

There are very few studies in the literature where chitosan or chitosan-based systems have been employed as direct active components or as carriers of antimicrobial systems in food packaging applications. Chi et al. reported the application of chitosan films containing oregano essential oil to bologna slices as a feasible antimicrobial packaging material for processed meat (*18*). Coma et al. described edible chitosan coatings with antimicrobial properties against *Listeria monocytogenes* and

* Corresponding author. E-mail: lagaron@iata.csic.es.
† Institute of Agrochemistry and Food Technology.
‡ University of Valencia.

10.1021/jf063110j CCC: $37.00
Published on Web 03/14/2007

made tests in Emmental cheese (*19*). Ouattara et al. studied the diffusion of acetic and propionic acids incorporated in chitosan films after immersion in water, and the effects of pH and temperature on diffusion were investigated (*20*). Songchai et al. studied vacuum-packaged chitosan coated grilled pork and reported that the chitosan coating was shown to minimize oxidation, as reflected by the peroxide values, color changes, and microbial counts of the samples (*6*). Vartiainen et al. reported a totally different system by which chitosan was immobilized onto plasma activated biaxially oriented polypropylene (BOPP) films to produce an active barrier that was reported to exhibit antimicrobial properties and an enhanced oxygen barrier (*21*). Li et al. developed glucomannan−chitosan−nisin ternary antimicrobial blends, in which the antimicrobial properties of the films were ascribed to the incorporation of nisin in the blend (*22*). Finally, Sebastien et al. developed antimicrobial chitosan/PLA-based bio-packaging that exhibited inhibitory effects against three fungi systems (*23*). In most cases, the reviewed studies dealt with the suitability of chitosan as a carrier for other antimicrobials or on the effects in food quality upon direct contact with the biopolymer. However, there is no previous work concerned with the actual mechanisms that play role when the natural biopolymer is directly used as an active packaging coating or discussion about how these can be controlled or monitored.

In this context, ATR-FTIR spectroscopy has become one of the most versatile techniques for the quick identification and characterization of substances because it gathers information from virtually any type of sample form and shape, provided that adequate accessories are employed, and furthermore, it can be used to, for instance, follow film forming processes and other in situ processes (*24*−*26*). This study shows relevant unprecedented work, and by the use of ATR-FTIR spectroscopy, it is shown how chitosonium acetate films behave in situ when they are put in contact with high relative humidity medium simulating solutions and high moisture foods and serves to put forward a novel and more efficient knowledge-based antimicrobial packaging design based on coatings of this versatile biopolymer.

EXPERIMENTAL PROCEDURES

Materials. A high molecular weight chitosan grade (reference number 419419) from Sigma-Aldrich Chemie (Steinhaim, Germany) with a viscosity of 1700 cps (at 1 wt % in 1 v % acetic acid) and coarse particle size that was obtained from crab shells was used. The molecular weight, M_w, of the polymer has been reported to range between 310×10^3 and 375×10^3, our specific grade being closer to the larger value since the measured viscosity is 1700 cps. The degree of deacetylation of the as-received chitosan was determined to be around 86% as estimated by FTIR methodology described in a previous work (*27*). No detectable crystallinity of the as-received material stored at 23 °C was observed by X-ray diffraction (using the synchrotron radiation soft condensed matter experimental setup described in ref 28) and calorimetry using a DSC 7 from Perkin-Elmer (Wellesley, MA).

Film Casting. A solution of chitosan flakes (1.5 wt % of chitosan in 0.5 and 2 v % aqueous acetic acid solution) was made and subsequently filtrated, and 60 μL of the filtrated solution was cast over the ATR crystal at controlled environmental conditions (i.e., 24 °C and 40% RH). Adhesion to the ATR upon drying was extremely good as judged by the excellent spectra recorded and by the difficulty in peeling off the formed film. The cast films were measured to have thicknesses of ca. 15 μm as determined by a micrometer after peeling off the films from the ATR equipment surface.

Solutions Used. A total of 15 μL of different water solutions, microbial solutions, nutrient solutions, and a film of tryptic soy agar (TSA) medium was deposited over the cast chitosonium acetate films, and ATR-FTIR spectra were recorded over time. The microbial solutions were MHB (Mueller−Hinton broth at pH 7.4) from Conda Laboratories (Madrid, Spain) containing a 10^5 CFU/mL mid-log phase culture of *Staphylococcus aureus* obtained from the Spanish-type culture collection. The nutrient solutions contained only MHB.

Wet Food Contact Simulation Medium. The TSA (Scharlau Chemie S.A., Barcelona, Spain) medium film was a very high humidity formulation that was thought to simulate high moisture foods such as fresh meats and contained casein peptone (15 g/L), soy peptone (5 g/L), sodium choride (5 g/L), and agar (15 g/L). To prepare the film, 40 g of the TSA powder was dissolved in 1 L of water, and then it was left to soak and was subsequently brought to boil and cast over Petri dishes to obtain a solid film during cooling that was stored at 35 °C overnight prior to its use.

Antimicrobial Tests. Supporting antimicrobial activity tests were performed by adding 0.06 g of the various high molecular weight chitosan samples (that had been obtained similarly as described previously but that were cast over Petri dishes) into a 10 mL of $10^5 \times$ CFU/mL mid-log phase culture of *S. aureus* and incubated at 37 °C for 24 h. The previous CFU counts were accurately and reproducibly obtained by inoculation of 0.1 mL of a culture with a 0.2 absorbance as determined by optical density at 600 nm by ultraviolet−visible (UV−vis) spectroscopy using a SP-2000 UV spectrometer (Spectrum Instruments company Ltd., Shanghai, China). Then, 0.1 mL of each MHB sample was sub-cultivated on the TSA plates. Finally, the plates were read after overnight incubation at 37 °C. These results were compared against both a control sample (MHB solution, pH 7.4) without chitosan and with a control sample containing MHB and were titrated with acetic acid to reach a pH of 5.74, which is similar to the pH of the chitosan solutions used for the casting of the films. Both controls reached, after incubation, microorganism counts of $4.4 \times 10^8 \pm 0.27$ and $1.2 \times 10^8 \pm 0.31$, respectively, clearly indicating the neither of the two controls exerted antimicrobial properties.

ATR-FTIR Spectroscopy. ATR-FTIR spectra were collected at 24 °C and 40% RH by coupling the ATR accessory GoldenGate of Specac Ltd. (Orpington, UK) to Bruker (Rheinstetten, Germany) FTIR Tensor 37 equipment. Time resolved experiments were collected by averaging, depending on the experiment, 10 or two scans at 4 cm^{-1} spectral resolution at predefined time intervals.

Modeling Diffusion Data. Data fitting to a suitable model are required to derive a quantitative measure of diffusion kinetics from experimental curves obtained using ATR-FTIR spectroscopy. To obtain D values from these sorption curves, the experimental curves must be fitted to the appropriated solution of Fick's second law of diffusion for the case of a plane sheet (eq 1) modified to suit an ATR experiment (eq 2) as proposed by Fieldson et al. (*29*)

$$\frac{M_t}{M_\infty} = 1 - \sum_{n=0}^{\infty} \frac{8}{(2n+1)^2\pi^2} \exp\left[\frac{-D(2n+1)^2\pi^2 t}{4L^2}\right] \quad (1)$$

$$\frac{A_t}{A_\infty} = 1 - \frac{8\gamma}{\pi[1-\exp(-2\gamma L)]} \sum_{n=0}^{\infty} \left[\frac{\exp\dfrac{-D(2n+1)^2\pi^2 t}{4L^2}\left[\dfrac{(2n+1)\pi}{2L}\exp(-2\gamma L) + (-1)^n(2\gamma)\right]}{(2n+1)\left(4\gamma^2 + \dfrac{(2n+1)\pi}{2L}\right)}\right] \quad (2)$$

where A_t and A_∞ are the spectral absorptions at a time t and equilibrium, respectively, d_p is the penetration depth, $\gamma = 1/d_p$, D is the diffusion coefficient, and L is the thickness of the coating.

However, in an analogous manner to that described in previous works (*29*−*32*), a simplified approach was used to determine D values (eq 3), which is based on an observed initial lag time (normalized to L), during which little sorption occurs within the evanescent field, followed

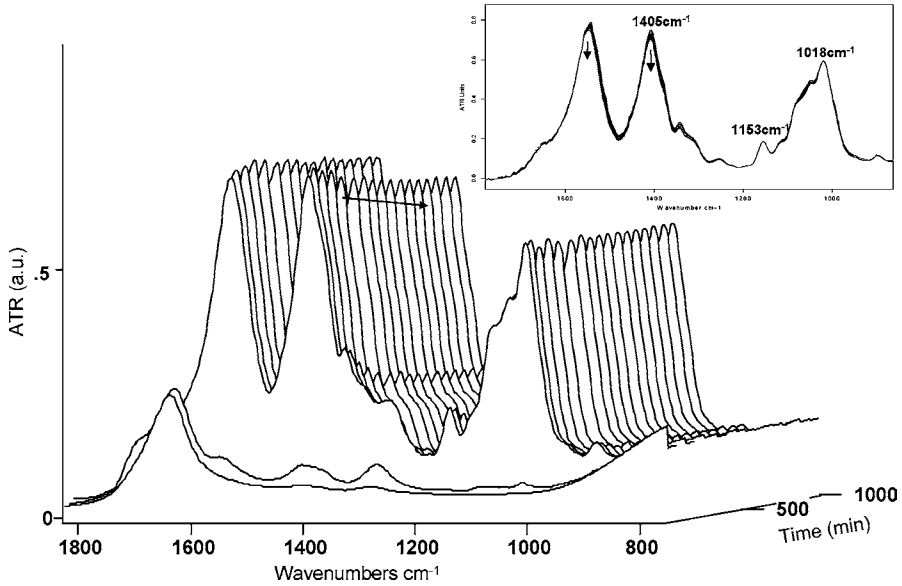

Figure 1. ATR-FTIR spectra evolution over time of the in situ studied film forming process of chitosan cast from a 2 wt % acetic acid solution. The inset shows only the overlapped spectra of this time evolution process recorded after complete film formation.

by a pseudo-Fickian ($\sqrt{t}$ power law) behavior predicted from eq 1 at short times

$$\frac{M_t}{M_\infty} = \frac{2}{L}\left(\frac{D}{\pi}\right)^n t^n \quad (3)$$

where $n = 0.5$.

The validity of D values derived from eq 3 is, similar to eq 2, strictly defined by the systems complying with Fick's laws of diffusion (eq 1). **Figure 6** indicates that the release of the biocide appears to be well-fitted by a Fickian model, and therefore, the application of eq 3 is justified. For a more extended discussion on this issue and on further instrumental considerations and formalisms for sorption-induced swelling systems, please see refs *29*−*32* and other cases discussed therein.

RESULTS AND DISCUSSION

ATR-FTIR spectroscopy was selected as a suitable tool to investigate the antimicrobial properties of chitosan because, even when other analytical tools can look into the release process of bioactive components in the liquid or food phase with perhaps higher sensitivity to trace levels, this vibrational spectroscopy technique is unique in that it can give direct information as to how the biocide and its chemistry is attached to the polymer matrix and is also able to fully, and simultaneously, characterize the whole release process, including chemical changes, sorption-induced swelling and release processes and their kinetics, and matrix phase and conformational changes (*29*−*32* and references therein).

Characterization of the Film Forming Process and of Its Environmental Aging. Figure 1shows some spectra (each being the average of 10 scans) taken during a real-time film forming process of a chitosan film cast from a 2% acetic acid solution directly over the ATR crystal.

As can be seen from the spectra evolution over time, the chitosonium acetate film was quickly formed after casting and evaporation of the solvent. At this step, the strong water band at 1638 cm^{-1} associated to OH in-plane bending and the free acetic acid band at 1706 cm^{-1} are no longer discerned in **Figure 1**, and only the typical bands arising from the chitosonium acetate compound become readily discerned in the spectrum of the solid state. Special mention should be made to the two bands arising from the carboxylate biocide groups ($-NH_3^+-OOCH$) at 1546 and at 1405 cm^{-1} (see arrows in the inset), which are not present in the as-received chitosan (see the bottom spectrum in **Figure 2**) (*33*). For a further and more detailed description of the chitosan and chitosonium acetate FTIR bands, please see refs *17* and *33*−*35*). For the sake of this study, it should be noted that during the evolution of the fully formed film over time (selected spectra in the inset of **Figure 1** where no free acetic acid band is seen), it is observed that at least two bands of the polymer remain largely unmodified (i.e., the bands at 1018 and 1153 cm^{-1}) and will consequently be used throughout this work as internal reference bands to account for absolute changes in the concentration of the carboxylate biocide groups. From **Figure 1**, it can be discerned that the carboxylate biocide groups are not stable in the environmental conditions of storage and that, following the first four spectra after solidification in **Figure 1**, in which the film is still being consolidated and the two bands still rise, a slight reduction in intensity of these two bands is observed over time in accordance with a previous study (see down arrows in the inset of **Figure 1**). The band intensity drop is known to be more acute in the 1405 cm^{-1} band, and therefore, this band has been previously used to monitor changes in the carboxylate groups in the polymer (*17*). The observations in **Figure 1** suggest that the chemistry of the chitosonium acetate film reverts progressively back to chitosan by dissolution in environmental humidity and subsequent evaporation in the form of acetic acid from the solid-state film. This is the so-called first mechanism (i.e., vaporization of acetic acid) that will be discussed in this study, by which the carboxylate biocide groups are being reduced inside the solid-state film. It should be stressed again that as the chitosonium acetate chemistry decreases in the film formulation, so does the expected biocide character of the active film (this will be further corroborated later in the paper).

Figure 2 shows the solid-state spectra of the two chitosonium acetate films obtained by casting from 0.5 and 2% acetic acid solutions of the biopolymer and the spectrum of the as-received chitosan.

From this figure, it can be easily observed that the as-received chitosan does not have carboxylate biocide groups in its chemistry as expected and that the film obtained using higher concentrations of the organic acid in the solution exhibits a

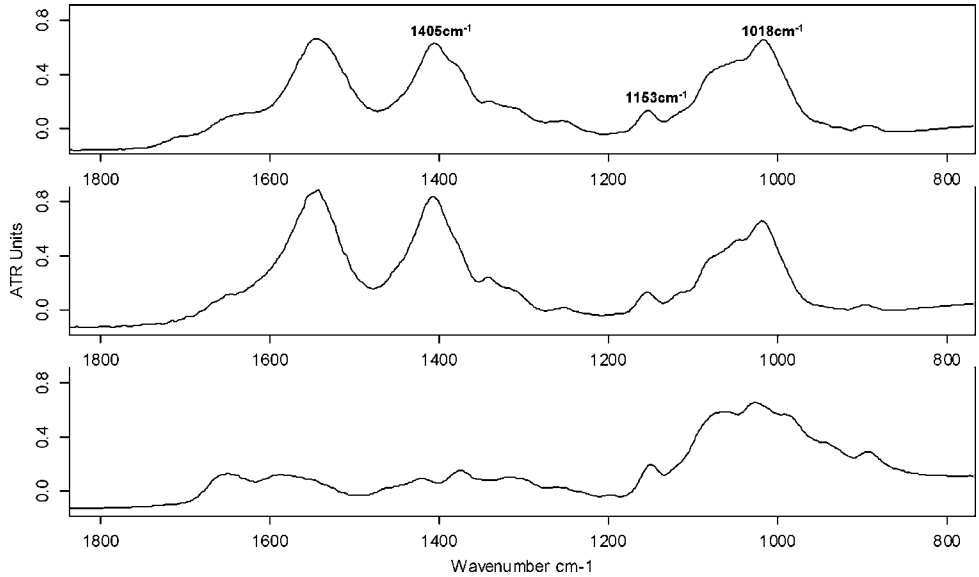

Figure 2. ATR-FTIR spectra taken in the film cast from a 2 wt % acetic acid solution (top spectrum), in the film cast from a 0.5 wt % acetic acid solution (middle spectrum), and in the as-received chitosan (bottom spectrum).

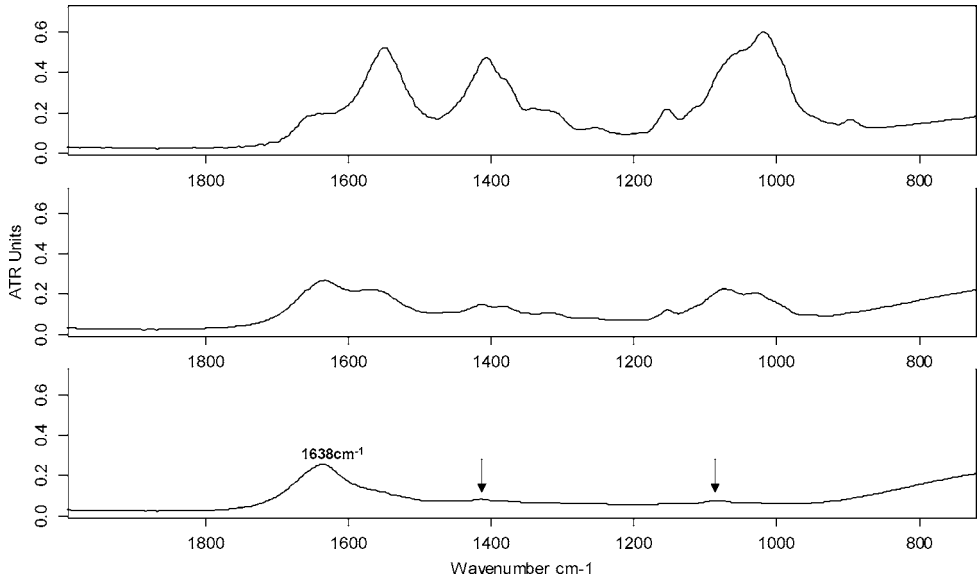

Figure 3. ATR-FTIR spectra taken in the film cast from a 0.5 wt % acetic acid solution (top spectrum), 5 s after contact with water (middle spectrum), and 10 s after contact with water (bottom spectrum).

higher intensity of the cited biocide groups as would also be expected. In light of previous work by Fernandez-Saiz et al. (*17*), reporting on antimicrobial results of various formulations of the current high molecular weight chitosan, the as-received chitosan should not exert a biocide character since it does not contain biocide groups, whereas the two cast films should do so.

Effect of Water and Microbial Solution Contact. Figure 3 gathers some selected spectra (each being the average of two scans) of the chitosonium acetate film cast from a 0.5% acetic acid solution when put in contact with water.

The first observation is that water diffuses so rapidly into the film that the first recorded spectrum (middle spectrum in **Figure 3** taken only 5 s after water deposition over the film surface) already shows a strong presence of the in-plane OH bending water band at 1638 cm^{-1} and a significant decrease in the polymer signal within the ATR evanescent field due to the concomitant polymer swelling/dissolution. More interestingly, however, is the observation that as moisture penetrates the sample, the cast film immediately releases a significant fraction of the carboxylate groups (see the relative intensity drop of the 1405 cm^{-1} band in the intermediate spectrum in **Figure 3** and the similarity of the spectrum with that of the as-received chitosan in **Figure 2**), which diffuse out rather immediately from the film into the upper liquid phase. The more heavily protonated amine molecules and/or the protonated lower molecular weight fractions (i.e., protonated glucosamine migrant groups) dissolve first from the film and diffuse more rapidly into the liquid phase. This does in turn suggest the existence of molecular heterogeneity at the molecular scale in the protonation of the amine chemistry and/or in the molecular weight within the polymer film. It is also interesting to note that even when the film has been fully soaked and the polymer signal diminishes by sorption of moisture—and, subsequently, polymer swelling and partial dissolution out of the evanescent field—the casting seems to still retain some of the polymer signal (see arrows), likely suggesting that part of the film still remains in a strongly plasticized hydrogel-like form as observed by visual inspection.

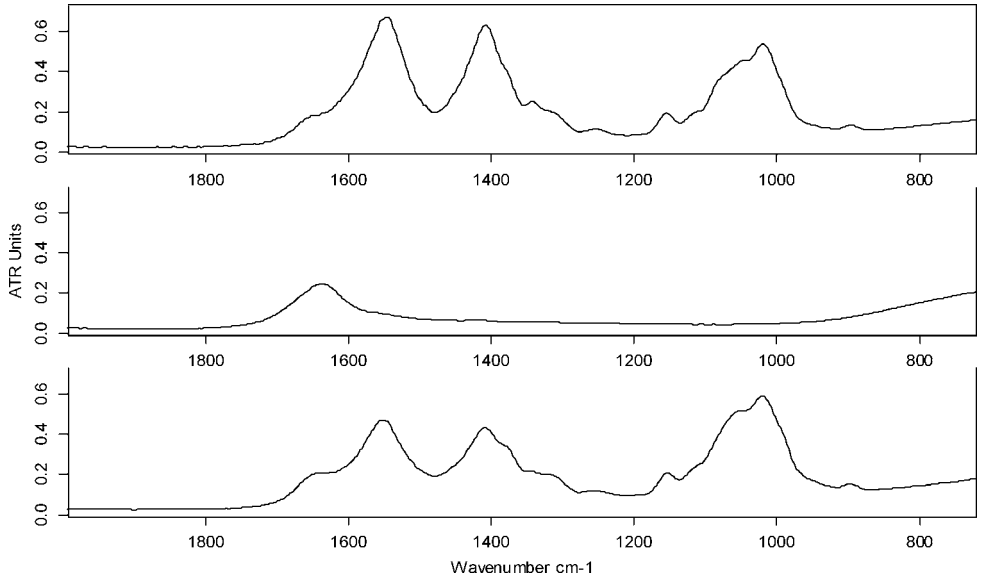

Figure 4. ATR-FTIR spectra taken in the film cast from a 2 wt % acetic acid solution (top spectrum), 5 s after contact with water (middle spectrum), and in the film redried after removal of deposited water with a pipet having been for 20 s in contact with the water solution (bottom spectrum).

It should be noted that the amount of liquid deposited was selected to yield swelling and plasticization of the film but not film dissolution. Thus, visual inspection indicated that the film was still attached to the ATR crystal mainly because the liquid was only deposited in a small area of the film surface on top of the ATR crystal. This event was further inferred by observation of the polymer signal in **Figure 3**. These results insightfully indicate that upon direct contact with humidity, the biocide carboxylate groups, which make up the water soluble fraction of the film, are immediately released from the film into the solvent phase and, therefore, that they are no longer retained in a solid-state form within the film. Previous work (*17*), and also **Figure 1**, pointed out that during film aging in the ATR cell at 24 °C and 40% RH, it is acetic acid that is being slowly vaporized into the medium. However, direct contact of the film with moisture suggests that the biocide chitosonium acetate in the form of protonated glucosamine fractions is primarily being released into the water medium, partially redissolving the film. This is further substantiated by results from previous works that unambiguously proved that protonated glucosamine groups easily migrated from similar chitosonium acetate films into the solution as measured by the colorimetric ninhydrin-based test, which is a specific test to evaluate primary amino groups in solution (*36*, *37*). The release of glucosamine groups is therefore referred to as the second mechanism (i.e., dissolution of protonated glucosamine groups to the liquid phase), by which the carboxylate biocide groups are being released from the solid-state film into the liquid contact medium.

The previously mentioned dual mechanism of release from the film, leading to decreased carboxylate groups in the solid-state chemistry, is a very important issue to be fully characterized and eventually understood, as it probably defines to a large extent the antimicrobial efficiency of the natural biopolymer. Thus, it seems that if water is in the vapor phase as environmental relative humidity (i.e., at water activities below 1), the mechanism of release is certainly the vaporization of acetic acid, not a strong antimicrobial agent in the concentrations used, given the lack of antimicrobial performance of the acetic acid control reported in the Experimental Procedures. Of course, relatively slow acetic acid vaporization in the absence of a liquid phase appears to be the only plausible mechanism because protonated glucosamine polymer segments cannot evaporate from the film. However, from **Figure 3** and the discussion that follows, direct contact with liquid phase water will additionally lead to a substantial dissolution and diffusion out of protonated amine groups from the film into the liquid phase, which are the most efficient biocide elements of chitosan and most likely directly responsible for its antimicrobial properties as suggested by a number of previous works discussed in the Introduction.

As mentioned previously, comparison of the middle spectrum in **Figures 3** and the bottom spectrum in **Figure 2** indicates that the spectrum of the remaining chitosonium acetate film immediately after contact with moisture becomes more similar to the as-received chitosan. Thus, in essence, the polymer signal in the medium and bottom spectra of **Figure 3** arising from within the evanescent field in direct contact with the ATR crystal points out that it is mainly non-water soluble chitosan that remains of the original cast film.

When similar cast films were put in contact with either the bacterial medium or with the nutrient medium, giving the water solution nature of these, similar results as with water were encountered, indicating that a positive migration process of the protonated glucosamine groups into the liquid phase occurs, which results in bacterial inactivation as will be seen later in the antimicrobial assays.

Figure 4 shows the spectra (each being the average of two scans) of the chitosonium acetate film cast from a 2% acetic acid solution when water was deposited on top of this. From this figure, it is observed that water diffusion and polymer extensive soaking and hydrogel formation takes place to a greater extent than in films with a lower concentration of protonated amine groups (i.e., cast from a 0.5 wt % acetic acid solution and with similar thickness). Thus, in the first registered spectrum (middle spectrum in **Figure 4** taken 5 s after water contact with the polymer surface), only the water band at 1638 cm^{-1} can be discerned. An interesting finding that corroborates the previous observations on the release of carboxylate biocide groups upon liquid phase contact is that, if after some water exposure (i.e., 20 s) the moisture is carefully removed from the top of the film with a pipet and the remaining biopolymer is allowed to re-dry, a film (see bottom spectrum in **Figure 4**) of chitosonium acetate resurfaces in the spectrum or reforms but with a lower intensity of the carboxylate bands, indicating that the film has lost biocide capacity as a result of diffusion of the

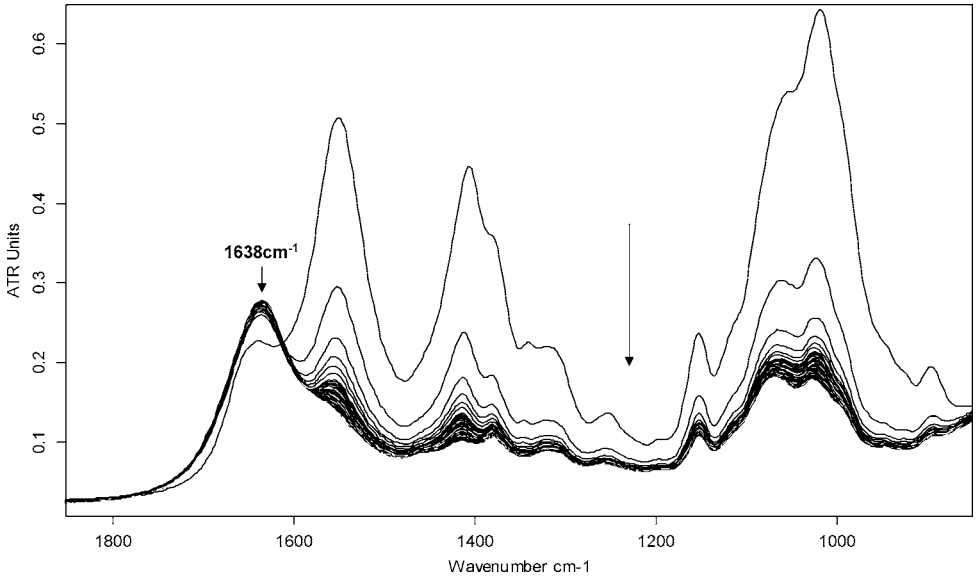

Figure 5. ATR-FTIR spectra recorded during the in situ direct contact of the chitosan film cast from a 0.5 wt % acetic acid solution with a highly moist TSA film medium. The arrow indicates the intensity evolution with increasing exposure time.

most soluble protonated glucosamine chain segments into the liquid phase during moisture exposure and their subsequent removal. Again, no differences were observed in the behavior of the chitosonium acetate film when the film was put in contact with the microbial or the nutrient solutions (i.e., the spectrum was immediately dominated by the sorbed moisture spectral features).

Effect of Wet Model Food Contact. At this point, it was clear that direct contact with water or water solutions was not going to provide sufficient insight into the release process of the biocide groups because of the very rapid and inhomogeneous diffusion kinetics of the moisture into the cast film. As a consequence, it was decided that instead of direct contact with water solution, it would perhaps be more advantageous to put the film into direct contact with a high moisture hydrogel medium such as TSA to, on the one hand, simulate direct contact with a fresh moisture food such as red meat and, on the other hand, to better resolve the diffusion process.

As anticipated, the TSA contact system allowed the recording (each spectrum being the average of two scans) of the sorption of moisture (presence of the 1632 cm^{-1} band), the concomitant polymer swelling (overall decrease in intensity of, i.e., the internal standard band at 1153 cm^{-1}), and the carboxylate biocide groups' release (relative drop in the 1405:1153 cm^{-1} intensity band ratio) with greater detail and time resolution (see **Figures 5** and **6**).

The spectral evolution in **Figure 5** clearly shows that initially a very fast sorption of water molecules takes place in the system, which progressively leads to the more simultaneous occurrence of polymer swelling and release of the biocide groups. This figure also shows that a larger quantity of the polymer remains within the evanescent field during the whole release process since water sorption does not so strongly take over the spectrum, possibly because of the presence of the TSA 500 μm thick film deposited on top of the cast chitosonium acetate film. The presence of the TSA film must lead to a more homogeneous behavior for the sorption of moisture as the process takes place more evenly across the chitosonium acetate casting and perhaps also imposes some constraints on the swelling of the underneath cast film, reducing overall swelling. In any case, what is clearly and insightfully observed is both the migration out of the evanescent field of the carboxylate groups and, as the protonated

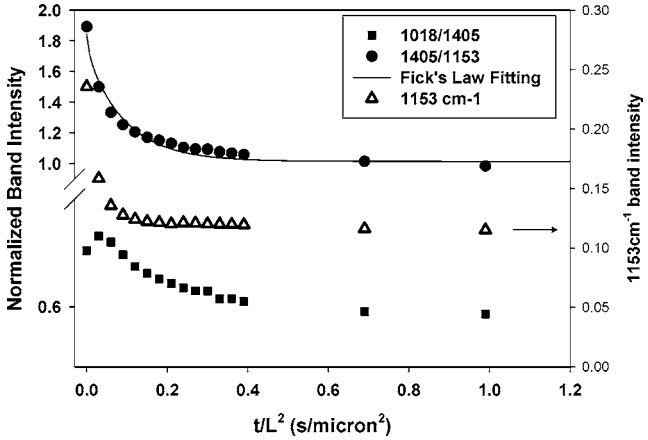

Figure 6. Normalized band intensity ratios 1018:1405 and 1405:1153 cm^{-1} and its Fick's law fitting to eq 1 in desorption and 1153 cm^{-1} band intensity over time/thickness^2 measured in the spectra of **Figure 5**.

glucosamine groups are drained out from the polymer, the film reverting back into a neutralized water insoluble chitosan formulation.

Figure 6 depicts the kinetics of the biocide groups' release process in the form of both the 1018:1405 and the 1405:1153 cm^{-1} band intensity ratios. The latter band ratio appears to yield more consistent data, including Fickian-like diffusion behavior, than the former and that makes the 1153 cm^{-1} band a more advisable internal standard for the polymer under the current study conditions. The reason for the 1018 cm^{-1} band giving less consistent data during this particular process is likely related to the significant shape changes experimented by the band envelope that contains this particular band during the migration of the carboxylate groups, which may be ascribed to concomitant conformational changes of the biopolymer (see also **Figure 2**). The estimated diffusion coefficient of the biocide groups' release obtained from application of eq 3 to the spectroscopic data in **Figure 6** is 3.67×10^{-12} m^2/s. **Figure 6** also depicts the mirroring concomitant drop in the polymer signal within the evanescent field revealed by the intensity drop of the 1153 cm^{-1} internal standard band, indicating that the protonated glucosamine release mechanism is induced by water sorption, subsequent polymer swelling, and partial dissolution as expected.

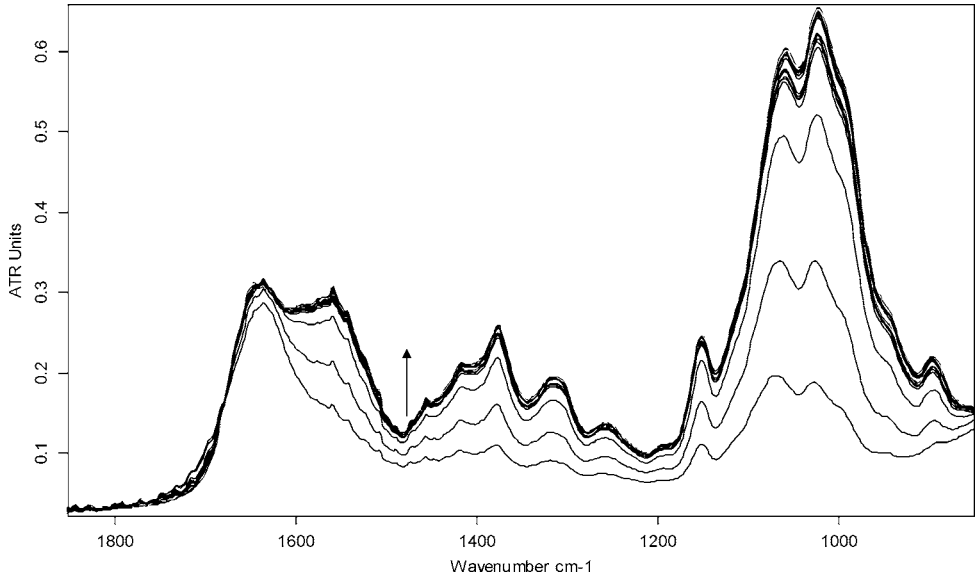

Figure 7. ATR-FTIR spectra recorded after removing the TSA medium from the cast chitosan film surface and showing the redrying process of the film in **Figures 5** and **6**. The arrow indicates the intensity evolution with increasing time.

The determination of whether the carboxylic groups are released during the TSA contact experiment in the form of acetic acid or in the form of protonated glucosamine groups (i.e., in the form of polymer migration) does not seen discernible from the FTIR spectra. However, after the experiment was finished, the TSA film was carefully removed from the surface of the cast film and allowed to dry (see **Figure 7**).

From comparison of these spectra with the spectrum of the as-received chitosan in **Figure 2**, it seems that the remaining film is clearly similar to the original as-received non-water soluble chitosan chemistry. Positive migration of glucosamine groups was also supported by the fact that some of the chitosonium acetate low viscosity hydrogel was visually stuck at the interphase of the two systems, indicating that no clear boundary between the two polymers occurred during removal and that they were interpenetrated. Thus, it becomes obvious that extensive polymer soaking, swelling, and partial dissolution has still taken place as in direct contact with water, and it is also very likely that migration of the most protonated soluble chain fragments has occurred on the surface of the TSA film. Evidently, it is anticipated that the lower the molecular weight of the starting chitosan polymer formulation, the faster and easier the migration and dispersion of the protonated groups into the moistured phase should be, due to the lower viscosity of the polymer. Further studies on other chitosan grades and on the role of polymer thickness, temperature, and additives such as nanoparticles of clays are being currently carried out in our labs to determine the effect of those on the migration process and will be reported elsewhere.

Antimicrobial Tests and Active Packaging Design. Figure 8 plots the antimicrobial results obtained in cast films of the various samples versus the calculated band intensity ratio 1405:1153 cm^{-1} per gram of used chitosan for the samples.

From these tests, it becomes clear that for samples with band intensity ratios above 27 g^{-1}, the chitosan formulation will exhibit biocide performance. Bacteriostatic effects are seen to occur at intensity ratios of ca. 27 g^{-1}, whereas for values above that, an increasing bactericide character is observed. The value of 27 g^{-1} was gathered from a film sample cast from a 0.5 wt % acetic acid solution, which underwent time aging at 24 °C and 60% RH before the antimicrobial test and that was obtained and reported in a previous work by Fernandez-Saiz et al. (*17*).

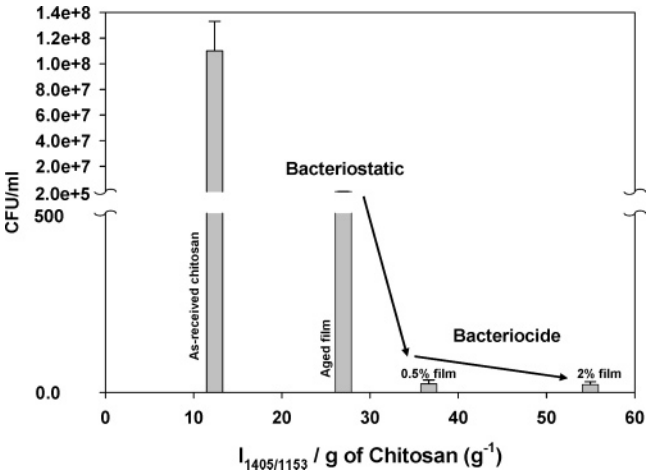

Figure 8. Colony forming units (CFU/mL) vs the normalized intensity of the 1405:1153 cm^{-1} band area ratio of, from left to right, as-received chitosan, an aged chitosan film described in ref *17*, a chitosan film cast from 0.5 wt % acetic acid solution, and a chitosan film cast from a 2 wt % acetic acid solution.

As the sample was aged, the number of carboxylic groups was reduced by evaporation in the form of acetic acid (just as can be observed in **Figure 1**) from the film and consequently only yielded bacteriostatic performance. The latter film did only show partial dissolution during the microbial tests. As reported previously, the as-received chitosan did not exhibit biocide properties as bacterial counts were similar to control values (see Experimental Procedures for control values). However, the two cast chitosonium acetate films readily redissolved when put in contact with the microbial solution and exhibited a strong biocide performance because as mentioned earlier and as can be observed in **Figure 8**, the characteristic band intensity ratios were higher than 27 g^{-1}. Acetic acid control solutions did not yield an antimicrobial performance as reported in the Experimental Procedures, suggesting that it is most likely that the presence of dissolved protonated glucosamine residues in direct contact with the cell medium is what is required to cause optimum microbial inactivation.

In summary, from the work described previously, it seems evident that the selected ATR-FTIR methodology provides

unique insight into the characterization of the antimicrobial process and properties of chitosan coatings; the thinner the coating, the more accurate the spectroscopic study, given the fact that the ATR-FTIR spectroscopy is primarily a surface measurement that provides information from typically 1 μm of the material. Of course, there is no fundamental reason to believe that in practice the behavior of the material within the evanescent field cannot be extended to the full coating thickness in a fully homogeneous sample. It is possible to argue, though, that as one needs a solution casting process to guarantee a good interfacial adhesion during the ATR experiment, the methodology may not be so accurate for the representation of melt process films or laminated coatings. Nevertheless, for solvent-based coatings, as is the case here, the methodology can be regarded as an excellent experimental recreation of a potential real antimicrobial coating application. In the case described here, the technique is also more suitable because it permits without disturbance us to have a unique perspective of the overall coating/food interaction processes when applied to real foodstuffs because the technique measures from below the coating to the food contact side.

From an active packaging development point of view, it also becomes evident that a sufficient number of carboxylate groups is needed in the packaging or food coating formulation (i.e., the film should stay above the 27 cm^{-1} value in the developed FTIR test). From our previous research, the coating should be kept in dry conditions prior to its use, to avoid losses of the biocide groups by organic acid evaporation in the presence of relative humidity. In the design of a chitosan-based active packaging system, it is envisaged that the chitosan active formulation should be included in the food contact layer as a coating. Another clear implication from the current research is that in the presence of moisture or in the highly wet conditions typically found in many foods, the biocide groups will be released very rapidly from the chitosan-based coating and will generate an immediate biocide effect at the surface and very possibly also underneath the surface, depending on the easiness of diffusion provided by the food matrix. However, if extended release is required, the chitosan-based active film should be blended with another more water resistant polymer (*37*) or biopolymer or protected by a controlled water permeability system like a porous or a highly plasticizable polymer or biopolymer matrix. It is evident that from the current research, it was learned that chitosan does act by contact in the presence of moisture, which leads to positive migration of biocide protonated glucosamine polymer chains into the moisture rich phase. Direct contact with moisture is needed because even when at low, medium, or medium-high relative humidity conditions, there is also migration of the organic acid to the vapor phase, and it has been found that the organic acid (see the acetic acid control test in the Experimental Procedures) is not a strong biocide in the concentrations used to generate the chitosonium acetate films. From a food quality (i.e., organoleptic, texture, etc.) perspective, it has been reported that chitosan does not adversely affect these properties (*6*). In this context, more compatible foods such as sea products, fish and seafood, could more strongly and directly benefit from the use of this material. However, it seems evident that the use of acetic acid in the formulation should be controlled and diminished to the furthest extent possible to optimize the active film formulation given the potential organoleptic impact of abuse of the latter element in the formulation. Another solution is to combine chitosan with other biocides as reported already in the literature to yield a stronger performance where needed; it seems evident from this work that the sorption-induced release capacity of entrapped molecules is expected to be very high in this material. Our group is currently working on several blend formulations of this biopolymer with other systems to tailor the performance over specific food products. With regard to the legislation aspects concerning the use of chitosan, it can be said that this biopolymer is already used as a food ingredient in Japan, whereas in Europe and in the U.S., it is currently used as a lipid trap in nutraceutical formulations (*38*). In Europe, the use of chitosan as a food ingredient is currently being reviewed.

LITERATURE CITED

(1) López-Rubio, A.; Almenar, E.; Hernandez-Muñoz, P.; Lagarón, J. M.; Catalá, R.; Gavara, R. Overview of active polymer-based packaging technologies for food applications. *Food Rev. Int.* **2004**, *20*, 357−387.

(2) Cooksey, K. Antimicrobial food packaging materials. *Additives for Polymers* **2001**, *8*, 6−10(5).

(3) Han, J. H. Antimicrobial food packaging. *Food Technol.* **2000**, *54*, 56−65.

(4) Labuza, T. P.; Breene, W. M. Application of active packaging for improvement of shelf-life and nutritional quality of fresh and extended shelf-life foods. *J. Food Process Preserv.* **1989**, *13*, 1−69.

(5) Hansen, R.; Rippl, C.; Miidkiff, D.; Neuwirth, J. Antimicrobial absorbent food pad. U.S. Patent 4-865-855, 1988.

(6) Yingyuad, S.; Ruamsin, S.; Reekprkhon, D.; Douglas, S.; Pongamphai, S.; Siripatrawan, U. Effect of chitosan coating and vacuum packaging on the quality of refrigerated grilled pork. *Packag. Technol. Sci.* **2006**, *19*, 149−157.

(7) Chung, Y.; Su, Y.; Chen, C.; Jia, G.; Wang, H.; Wu, J. C. G., Lin, J. Relationship between antibacterial activity of chitosan and surface characteristics of cell wall. *Acta Pharm. Sin.* **2004**, *25*, 932−936.

(8) Shahidi, F.; Abuzaytoun, A. R. Chitin, chitosan, and coproduce: Chemistry, production, applications, and health effects. *Adv. Food Nutr. Res.* **2005**, *49*, 94−135.

(9) Ralston, G. B.; Racey, M. V.; Wrench, P. M. Inhibition of fermentation in bakers yeast by chitosan. *Biochim. Biophys. Acta* **1964**, *93*, 652−655.

(10) Liu, H.; Du, Y.; Wang, X.; Sun, L. Chitosan kills bacteria through cell membrane damage. *Int. J. Food Microbiol.* **2004**, *95*, 147−155.

(11) Helander, I. M.; Nurmiaho-Lassila, E. L.; Ahvenainen, R.; Rhoades, J.; Roller, S. Chitosan disrupts the barrier properties of the outer membrane of Gram-negative bacteria. *Int. J. Food Microbiol.* **2001**, *71*, 235−244.

(12) Tokura, S.; Ueno, K.; Miyazaki, S.; Nishi, N. Molecular weight dependent antimicrobial activity by chitosan. *Macromol. Symp.* **1997**, *120*, 1−9.

(13) Hadwiger, L. A.; Kendra, D. F.; Fristensky, B. W.; Wagoner, W. Chitosan both activates genes in plants and inhibits RNA synthesis in fungi. In *Chitin in Nature and Technology*; Muzzarelli, R. A. A., Jeuniaux, C., Gooday, G. W., Eds.; Plenum Press: New York, 1985; pp 209−222.

(14) El Ghaouth, A.; Arul, J.; Asselin, A.; Benhamou, N. Antifungal activity of chitosan on post-harvest pathogens: Induction of morphological and cytological alterations in *Rhiuzopus stolonifer*. *Mycol. Res.* **1992**, *96*, 769−779.

(15) Cuero, R. G.; Osuji, G.; Washington, A. *N*-Carboxymethyl chitosan inhibition of aflatoxin production: Role of zinc. *Biotechnol. Lett.* **1991**, *13*, 441−444.

(16) Qin, C.; Li, H.; Xiao, Q.; Liu, Y.; Zhu, J.; Du, Y. Water solubility of chitosan and its antimicrobial activity. *Carbohydr. Polym.* **2006**, *63*, 367−374.

(17) Fernandez-Saiz, P.; Ocio, M. J.; Lagaron, J. M. Film forming process and biocide assessment of high molecular weight chitosan as determined by combined ATR-FTIR spectroscopy and antimicrobial assays. *Biopolymers* **2006**, *83* (6), 577−583.

(18) Chi, S.; Zivanovic, S.; Penfield, M. P. Application of chitosan films enriched with oregano essential oil on bologna—Active compounds and sensory attributes. *Food Sci. Technol. Int.* **2006**, *12*, 111−117.
(19) Coma, V.; Martial-Gros, A.; Garreau, S.; Copinet, A.; Salin, F.; Deschamps, A. Edible antimicrobial films based on chitosan matrix. *J. Food Sci*. **2002**, *67*, 1162−1169.
(20) Ouattara, B.; Simard, R. E.; Piette, G.; Begin, A.; Holley, R. A. Diffusion of acetic and propionic acids from chitosan-based antimicrobial packaging films. *J. Food Sci*. **2000**, *65*, 768−773.
(21) Vartiainena, J.; Rättöa, M.; Tapperb, U.; Paulussenc, S.; Hurmea, E. Surface modification of atmospheric plasma activated BOPP by immobilizing chitosan. *Polym. Bull.* **2005**, *54*, 343−352.
(22) Li, B.; Kennedy, J. F.; Peng, J. L.; Yi, X.; Xi, B. J. Preparation and performance evaluation of glucomannan−chitosan−nisin ternary antimicrobial blend film. *Carbohydr. Polym.* **2006**, *65*, 488−494.
(23) Sebastien, F.; Stephane, G.; Copinet, A.; Coma, V. Novel biodegradable films made from chitosan and poly(lactic acid) with antifungal properties against mycotoxinogen strains. *Carbohydr. Polym.* **2006**, *65*, 185−193.
(24) Hanh, B. D.; Neubert, R.; Wartewig, S. Investigations of drug release from suspensions using FTIR-ATR technique: Part I. Determination of effective diffusion coefficient of drugs. *Int. J. Pharm*. **2004**, *2000*, 145−150.
(25) Chan, K. L. A.; Kazarian, S. G. An innovative design of compaction cell for in situ FT-IR imaging of tablet dissolution. *Vib. Spectrosc.* **2004**, *35*, 45.
(26) Wartewig, S.; Neubert, R. H. H. Pharmaceutical applications of mid-IR and Raman spectroscopy. *Adv. Drug Delivery Rev.* **2005**, *57*, 1144−1170.
(27) Fernández-Cervera, M.; Heinämäki, J.; Räsänen, M.; Maunu, S. L.; Karjalainen, M.; Nieto-Acosta, O. M.; Iraizoz-Colarte, A.; Yliruusi, J. Solid-state characterization of chitosans derived from lobster chitin. *Carbohydr. Polym*. **2004**, *58*, 401−408.
(28) Lopez-Rubio, A.; Lagaron, J. M.; Gimenez, E.; Cava, D.; Hernandez-Muñoz, P.; Yamamoto, T.; Gavara, R. Morphological alterations induced by temperature and humidity in ethylene−vinyl alcohol copolymers. *Macromoleclues* **2003**, *36*, 9467−9476.
(29) Fieldson, G. T.; Barbari, A. T. The use of FTIR-ATR spectroscopy to characterize penetrant diffusion in polymers. *Polymer* **1993**, *34*, 1146.
(30) Döppers, L. M.; Breen, C.; Sammon, C. Diffusion of water and acetone into poly (vinyl alcohol)/clay nanocomposites using ATR-FTIR. *Vib. Spectrosc.* **2004**, *35*, 27−32.
(31) Cava, D.; Sammon, C.; Lagaron, J. M. Sorption-induced release of antimicrobial isopropanol in EVOH copolymers as determined by ATR-FTIR spectroscopy. *J. Appl. Polym. Sci*., **2007**, *103*, 3431−3437.
(32) Cava, D.; Sammon, C.; Lagaron, J. M. Water diffusion and sorption-induced swelling as a function of temperature and ethylene content in ethylene−vinyl alcohol copolymers as determined by attenuated total reflection Fourier transform infrared spectroscopy. *Appl. Spectrosc.* **2006**, *12*, 1392−1398.
(33) Zotkin, M. A.; Vikhoreva, G. A.; Kechekýan, A. S. Thermal modification of chitosan films in the form of salts with various acids. *Polym. Sci*. **2004**, *46*, 39−42.
(34) Osman, Z.; Arof, A. K. FTIR studies of chitosonium acetate-based polymer electrolytes. *Electrochim. Acta* **2003**, *48*, 993−999.
(35) Jae-Woon N.; Mi-Kyeong, J. Spectroscopic characterization and preparation of low molecular, water soluble chitosan with free amine group by novel methods. *J. Polym Sci., Part A: Polym. Chem.* **2002**, *40*, 3796−3803.
(36) Leane, M. M.; Nankervis, R.; Smith, A.; Illum, L. Use of ninhydrin assay to measure the release of chitosan from oral solid dosage forms. *Int. J. Pharm*. **2004**, *271*, 241−249.
(37) Fernandez-Saiz, P.; Hernandez-Muñoz, P.; Lagaron, J. M.; Ocio Zapata, M. J. *Antimicrobial Activity Evolution of Gliadin−Chitosonium Acetate Films for Food Packaging Applications*; Proceedings of the 2nd FEMS Congress of European Microbiologists: Madrid, Spain, 2006; p 192.
(38) Sebti, I.; Chollet, E.; Degraeve, C. N.; Peyrol, E. Water sensitivity, antimicrobial, and physicochemical analyses of edible films based on HPMC and/or chitosan. *J. Agric. Food Chem.* **2007**, *55*, 693−699.

Received for review October 28, 2006. Revised manuscript received February 1, 2007. Accepted February 10, 2007. The authors thank the MEC (Project MAT2006-10261-C03-01, -02, and -03), the EU Integrated Project SUSTAINPACK, and Nanobiomatters S.L. (Paterna, Spain) for financial support. Finally, P.F.-S. acknowledges the I3P postgraduate program of CSIC, Spain for financial support.

JF063110J